

# Observational Properties of Harmonic EMIC waves: Statistical Study

Shujie Gu<sup>1</sup>, Xu Liu<sup>1</sup>, Lunjin Chen<sup>1</sup>, M. E. Usanova<sup>2</sup>, Wenyao Gu<sup>1</sup>, Zhiyang Xia<sup>1</sup>

<sup>1</sup>William B. Hanson Center for Space Sciences, Department of Physics, University of Texas at Dallas,  
Richardson, Texas, USA

<sup>2</sup>Laboratory for Atmospheric and Space Physics, University of Colorado Boulder, Boulder, CO, USA

## Key Points:

- Harmonic EMIC waves concentrate outside the dayside plasmasphere at  $L > 5$ .
- Harmonic EMIC waves are associated with a low  $f_{pe}/f_{ce}$  and a high proton  $\beta_H$ .
- Most of the harmonic EMIC waves are accompanied by a strong EMIC fundamental mode.

arXiv:2412.16124v1 [physics.space-ph] 20 Dec 2024

---

Corresponding author: Shujie Gu and Xu Liu, [shujie.gu@utdallas.edu](mailto:shujie.gu@utdallas.edu); [xu.liu1@utdallas.edu](mailto:xu.liu1@utdallas.edu)

**Abstract**

Electromagnetic ion cyclotron (EMIC) waves are discrete electromagnetic emissions separated by multiple ion gyrofrequencies. Harmonic EMIC waves are defined as waves with a strong electric or magnetic field (or both) at the harmonics of the fundamental EMIC mode. In this paper, for the first time, we present a statistical study on harmonic EMIC waves by the Van Allen Probes. The EMIC waves are categorized into three types based on their harmonics: (1) fundamental mode only (without higher harmonics), (2) electrostatic (ES) harmonics, and (3) electromagnetic (EM) harmonics. Our statistical study shows that ES and EM harmonic EMIC waves predominantly occur on the dayside, outside the plasmasphere with  $L > 5$  and are associated with a low  $f_{pe}/f_{ce}$ , a high proton  $\beta_H$ , and a strong fundamental EMIC mode. The results will advance our understanding of harmonic EMIC waves and their generation mechanisms.

**Plain Language Summary**

Electromagnetic ion cyclotron (EMIC) waves play an essential role in the acceleration and precipitation of charged particles in the Earth's magnetosphere. They can resonate with MeV electrons and keV ions in the Earth's magnetosphere and produce the rapid loss of radiation belt electrons and ring current ions. EMIC waves are sometimes accompanied by electrostatic or electromagnetic harmonic structures in their frequency spectrum, though the properties of these harmonics remain poorly understood. In this paper, we present the first statistical study of harmonic EMIC waves with a narrow-band fundamental mode, as observed by the Van Allen Probes. Based on their harmonic structures, we categorize the EMIC wave events into three types: fundamental mode only (without harmonics), electrostatic (ES) harmonics, and electromagnetic (EM) harmonics. Our statistical study shows that ES and EM harmonic EMIC waves mainly concentrate on the dayside outside the plasmasphere with  $L > 5$  and are associated with a low  $f_{pe}/f_{ce}$ , a high proton  $\beta_H$ , and a strong fundamental mode. The statistical findings from these observations provide a foundation for further exploration of the mechanisms behind harmonic EMIC wave excitation.

**1 Introduction**

Electromagnetic ion cyclotron (EMIC) waves are electromagnetic emissions that occur within the Pc1-Pc2 geomagnetic pulsation frequency range, typically between 0.1 and 5 Hz (Allan & Poulter, 1992; Hartinger et al., 2022; Cornwall, 1965). They have been widely observed in the Earth magnetosphere (e.g., Anderson et al., 1990), solar wind (e.g., Jian et al., 2010), and other planets in the solar system (e.g., Barbosa, 1993; Boardson et al., 2012). Typical EMIC waves propagate in a quasi-parallel direction and exhibit left-hand polarization below ion cyclotron frequencies. In the presence of heavy ions, such as helium ( $\text{He}^+$ ) and oxygen ( $\text{O}^+$ ), magnetospheric EMIC waves can be divided into three bands: hydrogen, helium and oxygen bands, respectively (Koskinen & Kilpua, 2022). They can be excited by a pitch-angle anisotropy in energetic ions with energies of a few tens of keV (Gendrin et al., 1984; Jordanova et al., 2006), often caused by the injection of plasma sheet particles during geomagnetic storms (e.g., Chen et al., 2009, 2010), or by magnetospheric compression due to increased solar wind pressure or interplanetary shocks (e.g., Tsurutani et al., 2016; Yin et al., 2022; Usanova et al., 2010). EMIC waves preferentially occur in the afternoon sector near the magnetic equator (Allen et al., 2015) and on the dayside at large  $L$ -shells (Usanova et al., 2012). They become oblique along their propagation paths and undergo polarization reversal as the wave frequency crosses the crossover frequency at high latitudes (Fraser & Nguyen, 2001; Liu et al., 2013).

EMIC waves play a crucial role in the acceleration and precipitation of charged particles in the inner magnetosphere. They can resonate with relativistic ( $\sim$ MeV) electrons through the gyroresonance, leading to the rapid loss of radiation belt electrons (e.g., Thorne

& Kennel, 1971; Liu et al., 2012; Blum et al., 2015; Jordanova et al., 2008). Electrons with lower energies (tens to hundreds keV), can interact with EMIC waves via the bounce resonance, resulting in significant pitch angle scattering (Blum et al., 2019; Cao et al., 2017). In addition, EMIC waves can interact with ring current ions through gyroresonance and cause efficient ion precipitation (Jordanova et al., 2001, 2006). Recent studies have shown that EMIC waves can deplete radiation belt electrons and ring current ions simultaneously (e.g., Usanova et al., 2014; Lyu et al., 2022).

Recently, harmonic structures of EMIC waves have been reported. Zhu and Chen (2019) observed EMIC waves exhibiting strong electrostatic spectra at multiple and fractional frequencies of the fundamental EMIC waves. They proposed that these electrostatic harmonics are generated by wave-wave resonance between fundamental EMIC waves and an accompanying density mode, a density fluctuation caused by the compressional component of the wave's associated electric field. This mechanism was verified by using the cross-bicoherence of low-frequency EMIC waves, the density mode, and high-frequency EMIC waves. Moreover, Deng et al. (2022) observed harmonic EMIC waves with spectral peaks in both electric and magnetic fields, suggesting that higher-order harmonics are excited by wave-wave couplings between lower-order waves. They emphasized the key role of the second harmonic in this process, which has been supported by hybrid simulations and theoretical analysis (Xue et al., 2022; Yu et al., 2021).

Despite the case studies mentioned above, a comprehensive statistical analysis of harmonic EMIC waves remains lacking. In this paper, we utilize the Van Allen Probes data to conduct a statistical survey of harmonic EMIC waves characterized by the existence of electrostatic or electromagnetic harmonics and investigate their associated plasma conditions. Section 2 briefly introduces the Van Allen Probes data set and data methodology. The statistical results are presented in Section 3, followed by conclusions and discussions in Section 4.

## 2 Data Set and Methodology

We use data of the two Van Allen Probes from 2012 to 2019 to perform the statistical study. Magnetic field measurements are obtained from the Level-3 64 samples/s data in the Geocentric Solar Ecliptic (GSE) coordinate system, recorded by the fluxgate magnetometer sensor, part of the Electric and Magnetic Field Instrument Suite and Integrated Science (EMFISIS) suite (Kletzing et al., 2013). Electric field measurements are obtained from the Level-2 32 samples/s electric field data in the satellite's UVW coordinates, provided by the Electric Field and Waves (EFW) instrument (Wygant et al., 2013). The electric field measurement  $u$  and  $v$  components (in the spin plane) are used, and the  $w$  component along the spin axis is abandoned due to its high inaccuracy. We transform the magnetic fields into a field-aligned coordinate (FAC) system. The background magnetic field  $\mathbf{B}_0$  is calculated based on the time-averaged magnetic field data with a sliding window of 101 points, nearly 1.5 seconds. To calculate the electric and magnetic field spectra, we apply the fast Fourier transform (FFT) with a sliding window size of 1024-point time series and a 60-point overlap. The wave normal angles (WNAs) are determined through the singular value decomposition method (Santolík et al., 2003) based on the magnetic field.

Plasma density data are acquired from the Level-4 data, derived from the upper hybrid resonance frequency line identified from the electric field power spectrum by EMFISIS (Kurth et al., 2015). The plasmopause is treated as a boundary layer with a finite width. Thus, the inner magnetosphere is divided into three regions: inside the plasmasphere, outside the plasmasphere, and at the plasmasphere boundary layer (PBL). The PBL is determined based on the criteria in Liu et al. (2020) and Gu et al. (2022). Their method ensures that the PBLs are associated with sharp density gradients and pronounced density drops over  $L$ -shell, and only one PBL exists in each inbound or outbound

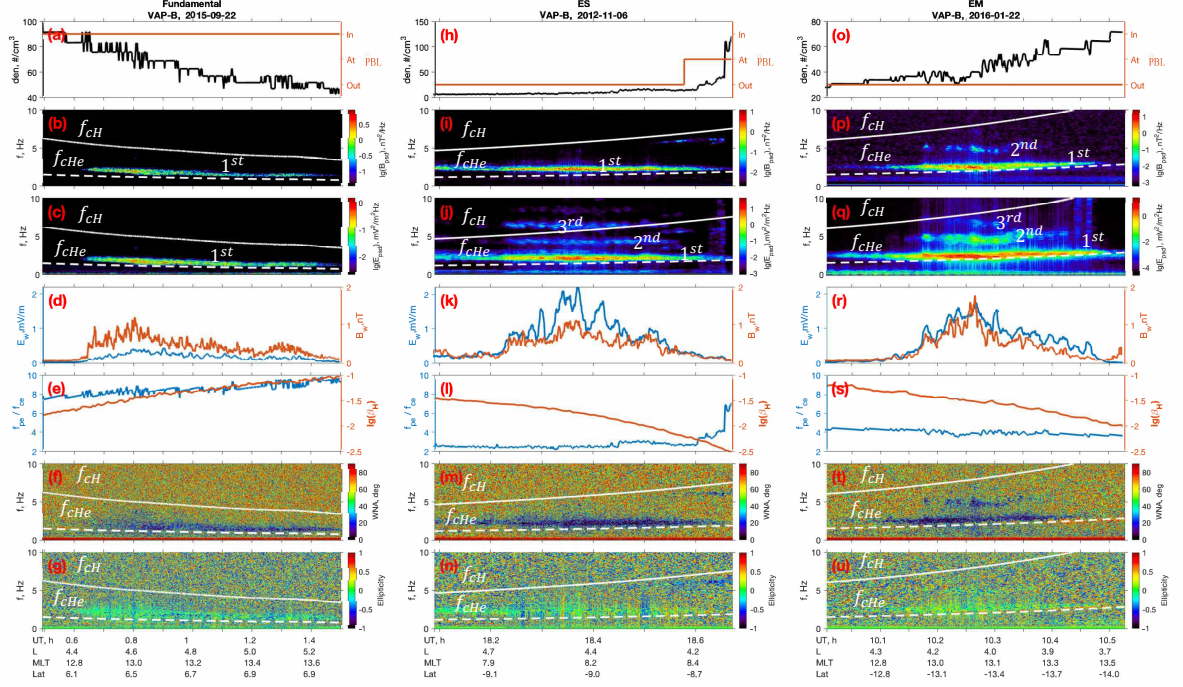


**Figure 1.** Three types of EMIC waves with only fundamental waves, electromagnetic (EM) harmonics, and electrostatic (ES) harmonics. (a, h, o): Background plasma density (in black) and satellite relative position to the PBL (in red). (b, i, p): Wave electric field power spectrum density. (c, j, q): Wave magnetic field power spectrum density. (d, k, r): Wave electric (in blue) and magnetic (in red) field magnitude. (e, l, s):  $f_{pe}/f_{ce}$  (in blue) and background plasma proton  $\beta$  (in red). (f, m, t): Wave normal angle. (g, n, u): Ellipticity. The white solid and dashed lines in subfigures represent the gyrofrequency of proton  $f_{cH+}$  and helium ion  $f_{cHe+}$ , respectively.

orbit. Ion pitch-angle distributions are derived from the differential flux measured by the Helium, Oxygen, Proton, and Electron (HOPE) Mass Spectrometer (Funsten et al., 2013; Spence et al., 2013). The ion temperature in an arbitrary direction is calculated as  $T = \frac{1}{n} \int f_i(\mathbf{v}) m_i v^2 d^3v$ , where  $n$  represents number density and  $f(\mathbf{v})$  is the phase space density in velocity space. The background plasma beta  $\beta$  is defined as the ratio of the plasma thermal pressure ( $p = nk_B T$ ) to the magnetic pressure ( $p_{mag} = B^2/2\mu_0$ ).

### 3 Results

We survey data from the Van Allen Probes throughout its mission (from 2012 to 2019) to identify EMIC wave events. We manually select events with narrow-band frequency, lasting at least five minutes, where the wave frequency remains nearly constant relative to the ion gyrofrequencies. These events are categorized into three types based on their harmonic properties: (1) fundamental-only (no higher harmonics), (2) electrostatic (ES) harmonics, and (3) electromagnetic (EM) harmonics. In this section, we first present three representative EMIC events observed by Van Allen Probe B (VAP-B), and then provide the statistical results based on the Van Allen Probes dataset.

Figure 1 shows examples of the three types of harmonic EMIC waves observed by Van Allen Probe (VAP-B). The left column (Fig 1a-1g) shows a fundamental harmonic EMIC wave event on September 22, 2015. Figure 1a shows the observed plasma density

(black) and relative relation to the PBL (red). The electric and magnetic field power spectral densities (PSDs) are presented in Figure 1b and 1c, respectively. A single narrow-band EMIC wave is observed with frequency close to the helium ion gyrofrequency  $f_{cHe+}$ , occurred inside the plasmasphere. The bandwidth  $\delta f$  is less than 0.5 Hz, and the ratio of the bandwidth to the proton gyrofrequency  $\delta f/f_{cH+}$  is smaller than 0.1. This type of EMIC wave is classified as a fundamental harmonic EMIC wave. In Figure 1d, we show the electric (blue) and magnetic (red) wave amplitudes. Figure 1e presents the ratio of the plasma frequency to the electron cyclotron frequency  $f_{pe}/f_{ce}$  with a value close to 10 (blue), and background proton beta  $\beta_H$  (red). They both slightly increase in this period. The WNAs are shown in Figure 1f, which indicates that these waves are nearly parallelly propagating. The wave polarization is primarily linear, as shown in Figure 1g. The middle column (Figure 1h-1n) show an ES harmonic EMIC wave event on November 16, 2012. The wave event is observed outside the plasmasphere during the VAP-B inbound pass at  $\sim 18.2$ -18.7 UT (Figure 1h). Compared to the fundamental case (Figure 1b and 1c), besides the fundamental mode, the electric field PSDs in Figure 1j have the second and third harmonic emissions. Since the high harmonics have no corresponding magnetic fluctuation, we classify this type of EMIC waves as an ES harmonic EMIC wave. The electric amplitude (Figure 1k) of this ES harmonic event (around 2 mV/m) is much larger than that (Figure 1d) of the fundamental event (around 0.2 mV/m). The  $f_{pe}/f_{ce}$  of the ES harmonic EMIC wave event (around 2, Figure 1l) is much smaller than that of the fundamental event (around 10, Figure 1e). Similar to the fundamental case, Figure 1m and 1n show the WNAs and wave ellipticity. In Figure 1o-1u, we show an EM harmonic EMIC wave event observed on January 22, 2016, which occurred outside the plasmasphere. Compared with the electric and magnetic PSDs of the fundamental and ES harmonic events (Figure 1b&c,i&j), the second harmonic exists in the magnetic field. We name this type of EMIC event as electromagnetic (EM) harmonic EMIC waves. Compared with the fundamental case in Figure 1d, the electric and magnetic field amplitudes are both larger in the EM harmonic case (Figure 1r).

We perform a statistical study to address the statistical characteristics of these three types of EMIC waves. In total, we identify 72 fundamental EMIC wave events, 85 ES harmonic EMIC events, and 53 EM harmonic EMIC wave events. For each event, we record the time corresponding to the maximum electric field amplitude. The distribution of events across  $L$ -shell and magnetic local time (MLT) is shown in Figure 2, where the terms “In”, “Out”, and “At” indicate the locations inside the plasmasphere, outside the plasmasphere, and at the PBL, respectively, as mentioned in the section 2. Figure 2a shows that over 60% of the fundamental EMIC waves occur inside the plasmasphere (blue asterisks) or at the PBL region (black circles), with no explicit dependency on the MLT. In contrast, Figure 2b and 2c demonstrate that more than 80% ES harmonic EMIC waves and nearly 70% EM harmonic EMIC waves happen outside the plasmasphere, with nearly 90% ES harmonic EMIC waves and 85% EM harmonic EMIC waves occurring on the dayside.

In Figure 3, we present the dependencies of EMIC events on the position and background plasma conditions. The probability in each bin is computed as the ratio of the number of events in each bin to the total number of events for each type. Figure 3a-3l illustrate the probability distribution of events based on their positions, including MLT, magnetic latitude (Mlat),  $L$ -shell, and their relation to PBL location. Figure 3a-3c show that both EM and ES harmonic EMIC waves are more concentrated on the dayside, mainly at 9-15 MLT, compared to the fundamental EMIC waves. In Figure 3d-3f, we find that these three types of events are most frequently observed near the geomagnetic equator. This trend is consistent with the excitation of EMIC waves near the equator due to the injection of anisotropic energetic ring current ions (Chen et al., 2010; Jordanova et al., 2008). Consequently, their harmonics, when present, are also expected to be predominantly located in the same region. Notably, EM harmonic EMIC waves occur more frequently near the equator compared to ES harmonic EMIC waves. Figure 3g shows that



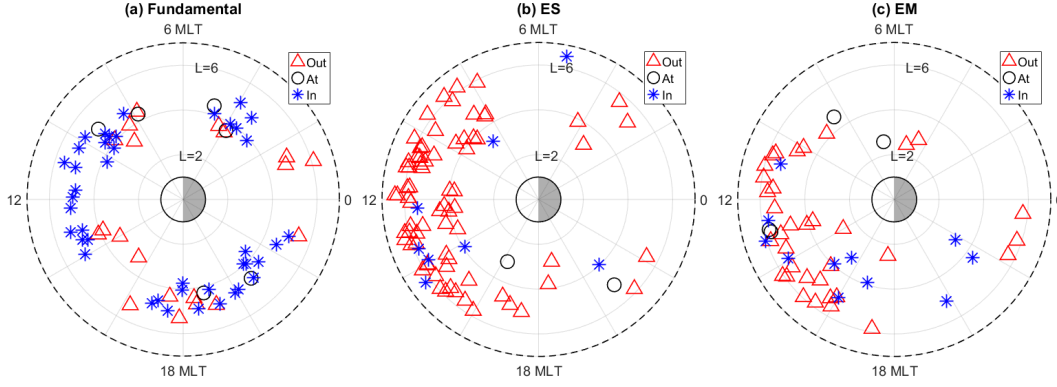


**Figure 2.** Event distributions across  $L$ -shell/MLT of: (a) Fundamental, (b) ES harmonic, and (c) EM harmonic EMIC events. The blue asterisks represent events inside the plasmasphere, the red triangles represent the events outside the plasmasphere, and the black circles represent the events at the PBL.

nearly 80% of fundamental EMIC events occur at  $L < 5$ , and 60% of these events take place inside the plasmasphere (Figure 3j). Conversely, more than 60% of ES and EM harmonic events are observed at  $L > 5$  (Figure 3h,i), and over 70% occur outside the plasmasphere (Figure 3k,l). Figure 3m-o and 3p-r show the dependencies on  $f_{pe}/f_{ce}$  and proton beta  $\beta_H$ . Compared with the fundamental events, the harmonic cases tend to occur with smaller  $f_{pe}/f_{ce}$  ( $< 9$ ) and larger proton  $\beta_H$  ( $> 0.1$ ). The mean values of these parameters of the three types of harmonic EMIC waves are summarized in Table 1. It shows the fundamental events have smaller  $L \sim 4.5$  and larger  $f_{pe}/f_{ce} \sim 10$ , while the harmonic events have larger  $L \sim 5$  and smaller  $f_{pe}/f_{ce} \sim 6$ .

Figure 4 summarizes the event dependencies of wave properties. Panels a-c and d-f display the probability distributions of wave electric field amplitude  $E_w$  and magnetic field amplitude  $B_w$ , respectively. Note that, even though the wave electric and magnetic amplitudes of EMIC harmonics are considerably large, they are still several orders of magnitude smaller than those of the fundamental modes. Thus, The wave electric and magnetic amplitudes here are mainly contributed from the fundamental mode. More than 85% ES and EM events are observed with  $E_w > 0.32$  mV/m and  $B_w > 0.32$  nT, whereas nearly 70% fundamental events happen with  $E_w < 0.32$  mV/m and  $B_w < 0.32$  nT. This indicates that both ES and EM harmonic EMIC events are associated with a stronger electromagnetic fundamental mode. Figure 4g-4i show the probability distributions of WNAs, revealing no significant differences in the WNA distributions among the three types of EMIC waves. In Table 1, the mean values of  $E_w$  and  $B_w$  support the conclusions drawn from the statistical results. Specifically, for ES harmonic events,  $E_w$  is nearly 10 times greater than that in the fundamental events, while  $B_w$  is nearly 2 times greater. For EM harmonic events,  $E_w$  is nearly 8 times greater, and  $B_w$  nearly 3 times greater compared to the fundamental events. The stronger fundamental mode in the harmonic event is aligned with previous studies (Zhu & Chen, 2019; Deng et al., 2022), indicating the nonlinear wave-wave excitation of the harmonic EMIC waves, which requires large amplitudes of fundamental waves.

## 4 Conclusions and Discussion

In this paper, we present, for the first time, a statistical study of the harmonic EMIC waves based on observations from the Van Allen Probes between 2012 and 2019. We focus on narrow-band EMIC waves, and categorize them into three groups based on the

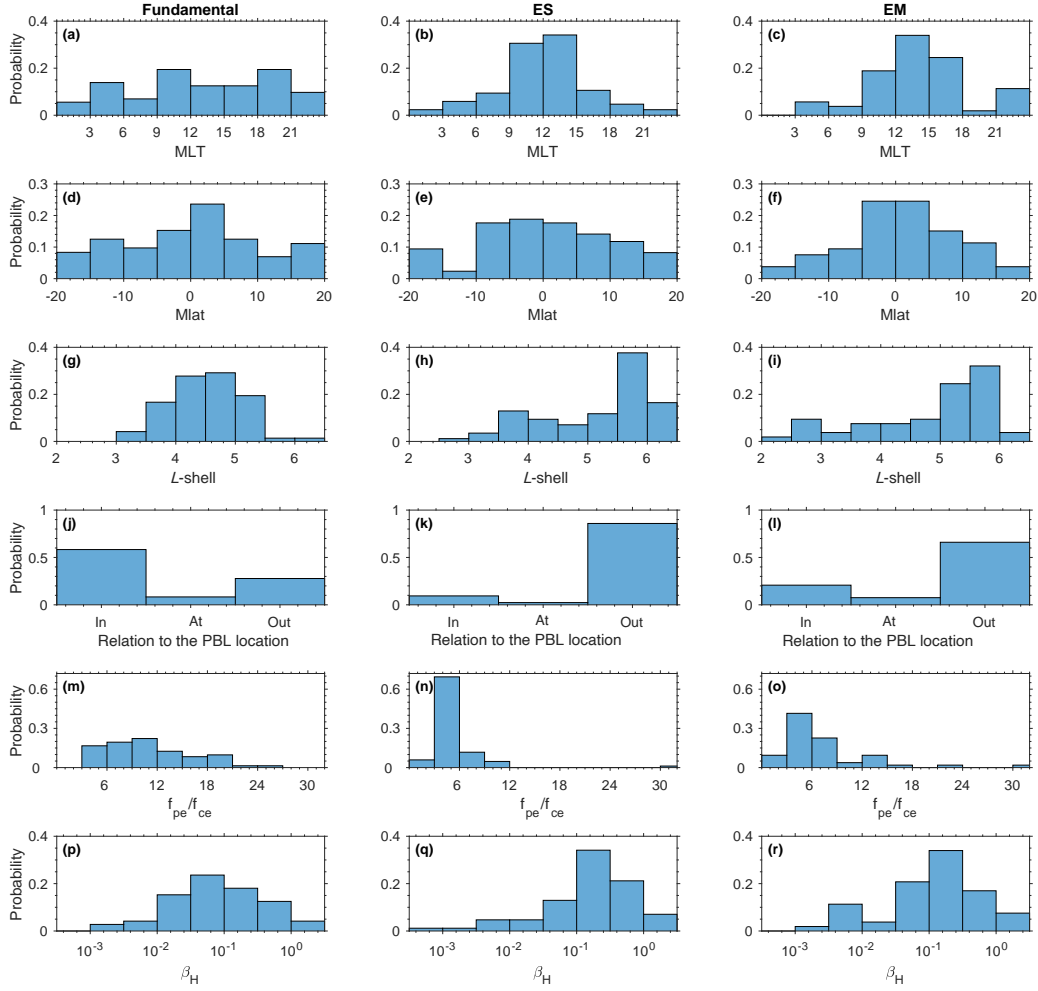


**Figure 3.** Statistical results of the position and plasma conditions of three types of EMIC waves. (a-c) Magnetic Local Time (MLT);(d-e) Magnetic latitude (Mlat); (g-i)  $L$ -shell; (j-l) The relative position to the PBL; (m-o)  $f_{pe}/f_{ce}$ ; (p-r) Proton beta  $\beta_H$ .

**Table 1.** Mean value of the parameters in Figure 3 and 4.

Parameters \ Categories	Fundamental	ES	EM
MLT(h)	12.96	12.26	13.96
Mlat(deg)	0.23	0.68	0.83
Lshell	4.5	5.18	4.86
$f_{pe}/f_{ce}$	10.00	6.03	5.89
$\log_{10}(\beta_H)$	-1.09	-0.83	-0.93
$E_w$ (mV/m)	0.31	2.93	2.56
$B_w$ (nT)	0.37	0.83	1.18
WNA(deg)	34.51	34.92	33.6

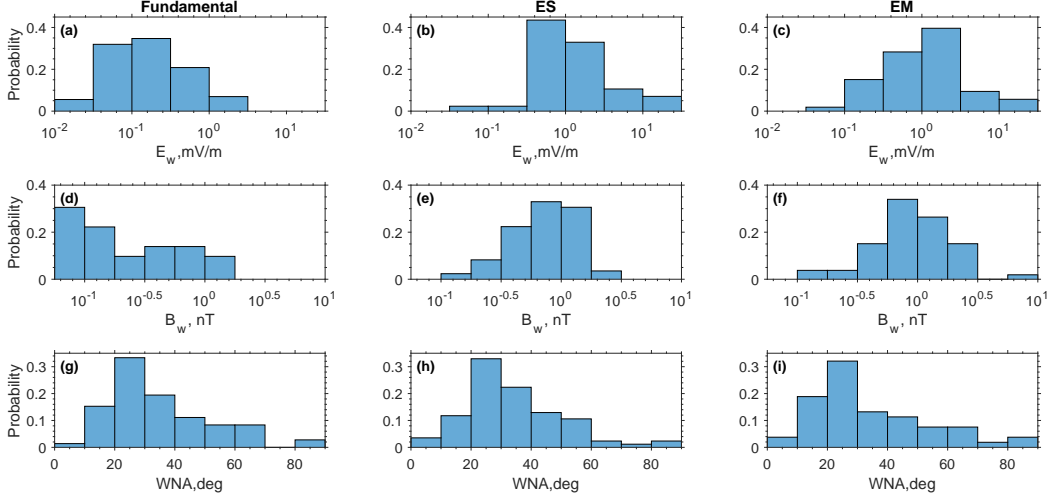


**Figure 4.** Statistical results of the wave properties of the fundamental mode of the three types of EMIC waves: (a-c) Wave electric field amplitude, (d-f) Wave magnetic field magnitude, and (g-i) Wave normal angle.

presence of harmonics. We then compare the properties of these three types of EMIC waves. The main conclusions are summarized as follows:

- (1) Harmonic EMIC waves are predominantly observed outside the dayside plasmasphere with  $L > 5$ .
- (2) Harmonic EMIC waves tend to occur in regions with a low  $f_{pe}/f_{ce}$  ( $< 9$ ) and a high proton  $\beta_H$  ( $> 0.1$ ).
- (3) Harmonic EMIC waves are mostly associated with strong fundamental modes ( $E_w > 0.32$  mV/m and  $B_w > 0.32$  nT), indicating nonlinear processes in the harmonic excitation.

For now, the statistical differences in wave properties between ES and EM cases are not prominent. The underlying mechanisms responsible for these two types of harmonic EMIC waves remain controversial. Some works suggested that nonlinear wave-wave coupling is responsible for exciting both two types of harmonic waves (e.g., Zhu & Chen, 2019; Deng et al., 2022). Sauer and Dubinin (2022) proposed that, in a multi-species plasma, energy and momentum exchange between different ion components could explain the origin of ES harmonic EMIC waves. Thus, identifying the distinct generation mechanisms behind these two types of waves will be the focus of our future work.

EMIC waves play a vital role in scattering electrons in the radiation belt, with previous studies primarily focusing on the interaction between electrons and monochromatic EMIC waves. An et al. (2014) proposed a two-wave model, showing that interactions with two-wave EMIC waves can induce more stochastic scattering of MeV electrons compared to single-wave interactions, as demonstrated through theory and test-particle simulations. In the future, we plan to investigate the response of electrons to harmonic EMIC waves, and compare this with their response to monochromatic EMIC waves based on observations.

This study confirms the existence of narrow-band intense EMIC waves. The higher harmonic components, when present, are significantly weaker than the fundamental component, but may still influence the saturation of the fundamental wave amplitude. Fu-



ture research, using particle-in-cell simulations, will aim to explore the underlying non-linear physics involved in these processes.

## Open Research Section

The data of Van Allen Probes used in this paper are provided by the Space Physics Data Facility (SPDF) (<https://spdf.gsfc.nasa.gov/pub/data/rbsp/>). The EMIC wave event list used in this paper is in the dataset (?, ?).

## Acknowledgments

We acknowledge the support of NASA Grant 80NSSC19K0283, 80NSSC21K0518.

## References

- Allan, W., & Poulter, E. M. (1992, may). Ulf waves-their relationship to the structure of the earth's magnetosphere. *Reports on Progress in Physics*, 55(5), 533. Retrieved from <https://dx.doi.org/10.1088/0034-4885/55/5/001> doi: 10.1088/0034-4885/55/5/001
- Allen, R. C., Zhang, J.-C., Kistler, L. M., Spence, H. E., Lin, R.-L., Klecker, B., ... Jordanova, V. K. (2015). A statistical study of emic waves observed by cluster: 1. wave properties. *Journal of Geophysical Research: Space Physics*, 120(7), 5574-5592. Retrieved from <https://agupubs.onlinelibrary.wiley.com/doi/abs/10.1002/2015JA021333> doi: <https://doi.org/10.1002/2015JA021333>
- An, X., Chen, L., Bortnik, J., & Thorne, R. M. (2014). An oscillator model representative of electron interactions with emic waves. *Journal of Geophysical Research: Space Physics*, 119(3), 1951-1959. Retrieved from <https://agupubs.onlinelibrary.wiley.com/doi/abs/10.1002/2013JA019597> doi: <https://doi.org/10.1002/2013JA019597>
- Anderson, B. J., Takahashi, K., Erlandson, R. E., & Zanetti, L. J. (1990). Pc1 pulsations observed by ampte/cce in the earth's outer magnetosphere. *Geophysical Research Letters*, 17(11), 1853-1856. Retrieved from <https://agupubs.onlinelibrary.wiley.com/doi/abs/10.1029/GL017i011p01853> doi: <https://doi.org/10.1029/GL017i011p01853>
- Barbosa, D. D. (1993). Theory and observations of electromagnetic ion cyclotron waves in saturn's inner magnetosphere. *Journal of Geophysical Research: Space Physics*, 98(A6), 9345-9350. Retrieved from <https://agupubs.onlinelibrary.wiley.com/doi/abs/10.1029/93JA00476> doi: <https://doi.org/10.1029/93JA00476>
- Blum, L., Artemyev, A., Agapitov, O., Mourenas, D., Boardsen, S., & Schiller, Q. (2019). Emic wave-driven bounce resonance scattering of energetic electrons in the inner magnetosphere. *Journal of Geophysical Research: Space Physics*, 124(4), 2484-2496. Retrieved from <https://agupubs.onlinelibrary.wiley.com/doi/abs/10.1029/2018JA026427> doi: <https://doi.org/10.1029/2018JA026427>
- Blum, L. W., Halford, A., Millan, R., Bonnell, J. W., Goldstein, J., Usanova, M., ... Li, X. (2015). Observations of coincident emic wave activity and duskside energetic electron precipitation on 18-19 january 2013. *Geophysical Research Letters*, 42(14), 5727-5735. Retrieved from <https://agupubs.onlinelibrary.wiley.com/doi/abs/10.1002/2015GL065245> doi: <https://doi.org/10.1002/2015GL065245>
- Boardsen, S. A., Slavin, J. A., Anderson, B. J., Korth, H., Schriver, D., & Solomon, S. C. (2012). Survey of coherent 1 hz waves in mercury's inner magnetosphere from messenger observations. *Journal of Geophysical Research: Space Physics*,

- 117(A12). Retrieved from <https://agupubs.onlinelibrary.wiley.com/doi/abs/10.1029/2012JA017822> doi: <https://doi.org/10.1029/2012JA017822>
- Cao, X., Ni, B., Summers, D., Bortnik, J., Tao, X., Shprits, Y. Y., ... Wang, Q. (2017). Bounce resonance scattering of radiation belt electrons by h+ band emic waves. *Journal of Geophysical Research: Space Physics*, 122(2), 1702-1713. Retrieved from <https://agupubs.onlinelibrary.wiley.com/doi/abs/10.1002/2016JA023607> doi: <https://doi.org/10.1002/2016JA023607>
- Chen, L., Thorne, R. M., & Horne, R. B. (2009). Simulation of emic wave excitation in a model magnetosphere including structured high-density plumes. *Journal of Geophysical Research: Space Physics*, 114(A7). Retrieved from <https://agupubs.onlinelibrary.wiley.com/doi/abs/10.1029/2009JA014204> doi: <https://doi.org/10.1029/2009JA014204>
- Chen, L., Thorne, R. M., Jordanova, V. K., Wang, C.-P., Gkioulidou, M., Lyons, L., & Horne, R. B. (2010). Global simulation of emic wave excitation during the 21 april 2001 storm from coupled rcm-ram-hotray modeling. *Journal of Geophysical Research: Space Physics*, 115(A7). Retrieved from <https://agupubs.onlinelibrary.wiley.com/doi/abs/10.1029/2009JA015075> doi: <https://doi.org/10.1029/2009JA015075>
- Cornwall, J. M. (1965). Cyclotron instabilities and electromagnetic emission in the ultra low frequency and very low frequency ranges. *Journal of Geophysical Research (1896-1977)*, 70(1), 61-69. Retrieved from <https://agupubs.onlinelibrary.wiley.com/doi/abs/10.1029/JZ070i001p00061> doi: <https://doi.org/10.1029/JZ070i001p00061>
- Deng, D., Yuan, Z., Huang, S., Xue, Z., Huang, Z., & Yu, X. (2022). Electromagnetic ion cyclotron harmonic waves generated via nonlinear wave-wave couplings. *Geophysical Research Letters*, 49(4), e2021GL097143. Retrieved from <https://agupubs.onlinelibrary.wiley.com/doi/abs/10.1029/2021GL097143> (e2021GL097143 2021GL097143) doi: <https://doi.org/10.1029/2021GL097143>
- Fraser, B., & Nguyen, T. (2001). Is the plasmopause a preferred source region of electromagnetic ion cyclotron waves in the magnetosphere? *Journal of Atmospheric and Solar-Terrestrial Physics*, 63(11), 1225-1247. Retrieved from <https://www.sciencedirect.com/science/article/pii/S13646826000225X> (The Plasmasphere Revisited: A Tribute to Donald Carpenter) doi: [https://doi.org/10.1016/S1364-6826\(00\)00225-X](https://doi.org/10.1016/S1364-6826(00)00225-X)
- Funsten, H. O., Skoug, R. M., Guthrie, A. A., MacDonald, E. A., Baldonado, J. R., Harper, R. W., ... Chen, J. (2013, Nov 01). Helium, oxygen, proton, and electron (hope) mass spectrometer for the radiation belt storm probes mission. *Space Science Reviews*, 179(1), 423-484. Retrieved from <https://doi.org/10.1007/s11214-013-9968-7> doi: 10.1007/s11214-013-9968-7
- Gendrin, R., Ashour-Abdalla, M., Omura, Y., & Quest, K. (1984). Linear analysis of ion cyclotron interaction in a multicomponent plasma. *Journal of Geophysical Research: Space Physics*, 89(A10), 9119-9124. Retrieved from <https://agupubs.onlinelibrary.wiley.com/doi/abs/10.1029/JA089iA10p09119> doi: <https://doi.org/10.1029/JA089iA10p09119>
- Gu, W., Liu, X., Xia, Z., & Chen, L. (2022). Statistical study on small-scale ( $\leq 1,000$  km) density irregularities in the inner magnetosphere. *Journal of Geophysical Research: Space Physics*, 127(7), e2022JA030574. Retrieved from <https://agupubs.onlinelibrary.wiley.com/doi/abs/10.1029/2022JA030574> (e2022JA030574 2022JA030574) doi: <https://doi.org/10.1029/2022JA030574>
- Hartinger, M. D., Takahashi, K., Drozdov, A. Y., Shi, X., Usanova, M. E., & Kress, B. (2022). Ulf wave modeling, effects, and applications: Accomplishments, recent advances, and future. *Frontiers in Astronomy and Space Sciences*, 9. Retrieved from <https://www.frontiersin.org/articles/10.3389/>

- fspas.2022.867394 doi: 10.3389/fspas.2022.867394
- Jian, L. K., Russell, C. T., Luhmann, J. G., Anderson, B. J., Boardsen, S. A., Strangeway, R. J., ... Wennmacher, A. (2010). Observations of ion cyclotron waves in the solar wind near 0.3 au. *Journal of Geophysical Research: Space Physics*, 115(A12). Retrieved from <https://agupubs.onlinelibrary.wiley.com/doi/abs/10.1029/2010JA015737> doi: <https://doi.org/10.1029/2010JA015737>
- Jordanova, V. K., Albert, J., & Miyoshi, Y. (2008). Relativistic electron precipitation by emic waves from self-consistent global simulations. *Journal of Geophysical Research: Space Physics*, 113(A3). Retrieved from <https://agupubs.onlinelibrary.wiley.com/doi/abs/10.1029/2008JA013239> doi: <https://doi.org/10.1029/2008JA013239>
- Jordanova, V. K., Farrugia, C. J., Thorne, R. M., Khazanov, G. V., Reeves, G. D., & Thomsen, M. F. (2001). Modeling ring current proton precipitation by electromagnetic ion cyclotron waves during the may 14–16, 1997, storm. *Journal of Geophysical Research: Space Physics*, 106(A1), 7-22. Retrieved from <https://agupubs.onlinelibrary.wiley.com/doi/abs/10.1029/2000JA002008> doi: <https://doi.org/10.1029/2000JA002008>
- Jordanova, V. K., Miyoshi, Y. S., Zaharia, S., Thomsen, M. F., Reeves, G. D., Evans, D. S., ... Fennell, J. F. (2006). Kinetic simulations of ring current evolution during the geospace environment modeling challenge events. *Journal of Geophysical Research: Space Physics*, 111(A11). Retrieved from <https://agupubs.onlinelibrary.wiley.com/doi/abs/10.1029/2006JA011644> doi: <https://doi.org/10.1029/2006JA011644>
- Kletzing, C. A., Kurth, W. S., Acuna, M., MacDowall, R. J., Torbert, R. B., Averkamp, T., ... Tyler, J. (2013, Nov 01). The electric and magnetic field instrument suite and integrated science (emfisis) on rbsp. *Space Science Reviews*, 179(1), 127-181. Retrieved from <https://doi.org/10.1007/s11214-013-9993-6> doi: 10.1007/s11214-013-9993-6
- Koskinen, H., & Kilpua, E. (2022). *Physics of earth's radiation belts: Theory and observations*. Switzerland: Springer Nature Switzerland AG. doi: 10.1007/978-3-030-82167-8
- Kurth, W. S., De Pascuale, S., Faden, J. B., Kletzing, C. A., Hospodarsky, G. B., Thaller, S., & Wygant, J. R. (2015). Electron densities inferred from plasma wave spectra obtained by the waves instrument on van allen probes. *Journal of Geophysical Research: Space Physics*, 120(2), 904-914. Retrieved from <https://agupubs.onlinelibrary.wiley.com/doi/abs/10.1002/2014JA020857> doi: <https://doi.org/10.1002/2014JA020857>
- Liu, K., Winske, D., Gary, S. P., & Reeves, G. D. (2012). Relativistic electron scattering by large amplitude electromagnetic ion cyclotron waves: The role of phase bunching and trapping. *Journal of Geophysical Research: Space Physics*, 117(A6). Retrieved from <https://agupubs.onlinelibrary.wiley.com/doi/abs/10.1029/2011JA017476> doi: <https://doi.org/10.1029/2011JA017476>
- Liu, X., Chen, L., & Xia, Z. (2020). The relation between electron cyclotron harmonic waves and plasmopause: Case and statistical studies. *Geophysical Research Letters*, 47(9), e2020GL087365. Retrieved from <https://agupubs.onlinelibrary.wiley.com/doi/abs/10.1029/2020GL087365> (e2020GL087365 10.1029/2020GL087365) doi: <https://doi.org/10.1029/2020GL087365>
- Liu, Y. H., Fraser, B. J., & Menk, F. W. (2013). Emic waves observed by cluster near the plasmopause. *Journal of Geophysical Research: Space Physics*, 118(9), 5603-5615. Retrieved from <https://agupubs.onlinelibrary.wiley.com/doi/abs/10.1002/jgra.50486> doi: <https://doi.org/10.1002/jgra.50486>
- Lyu, X., Ma, Q., Tu, W., Li, W., & Capannolo, L. (2022). Modeling the simultane-

- ous dropout of energetic electrons and protons by emic wave scattering. *Geophysical Research Letters*, *49*(20), e2022GL101041. Retrieved from <https://agupubs.onlinelibrary.wiley.com/doi/abs/10.1029/2022GL101041> (e2022GL101041 2022GL101041) doi: <https://doi.org/10.1029/2022GL101041>
- Santolík, O., Parrot, M., & Lefeuvre, F. (2003). Singular value decomposition methods for wave propagation analysis. *Radio Science*, *38*(1). Retrieved from <https://agupubs.onlinelibrary.wiley.com/doi/abs/10.1029/2000RS002523> doi: <https://doi.org/10.1029/2000RS002523>
- Sauer, K., & Dubinin, E. (2022). Multi-ion oscillitons—origin of coherent magnetospheric emic waves. *Journal of Geophysical Research: Space Physics*, *127*(10), e2022JA030925. Retrieved from <https://agupubs.onlinelibrary.wiley.com/doi/abs/10.1029/2022JA030925> (e2022JA030925 2022JA030925) doi: <https://doi.org/10.1029/2022JA030925>
- Spence, H. E., Reeves, G. D., Baker, D. N., Blake, J. B., Bolton, M., Bourdarie, S., ... Thorne, R. M. (2013, Nov 01). Science goals and overview of the radiation belt storm probes (rbsp) energetic particle, composition, and thermal plasma (ect) suite on nasa's van allen probes mission. *Space Science Reviews*, *179*(1), 311-336. Retrieved from <https://doi.org/10.1007/s11214-013-0007-5> doi: [10.1007/s11214-013-0007-5](https://doi.org/10.1007/s11214-013-0007-5)
- Thorne, R. M., & Kennel, C. F. (1971). Relativistic electron precipitation during magnetic storm main phase. *Journal of Geophysical Research (1896-1977)*, *76*(19), 4446-4453. Retrieved from <https://agupubs.onlinelibrary.wiley.com/doi/abs/10.1029/JA076i019p04446> doi: <https://doi.org/10.1029/JA076i019p04446>
- Tsurutani, B. T., Hajra, R., Tanimori, T., Takada, A., Remya, B., Mannucci, A. J., ... Gonzalez, W. D. (2016). Heliospheric plasma sheet (hps) impingement onto the magnetosphere as a cause of relativistic electron dropouts (reds) via coherent emic wave scattering with possible consequences for climate change mechanisms. *Journal of Geophysical Research: Space Physics*, *121*(10), 10,130-10,156. Retrieved from <https://agupubs.onlinelibrary.wiley.com/doi/abs/10.1002/2016JA022499> doi: <https://doi.org/10.1002/2016JA022499>
- Usanova, M. E., Drozdov, A., Orlova, K., Mann, I. R., Shprits, Y., Robertson, M. T., ... Wygant, J. (2014). Effect of emic waves on relativistic and ultrarelativistic electron populations: Ground-based and van allen probes observations. *Geophysical Research Letters*, *41*(5), 1375-1381. Retrieved from <https://agupubs.onlinelibrary.wiley.com/doi/abs/10.1002/2013GL059024> doi: <https://doi.org/10.1002/2013GL059024>
- Usanova, M. E., Mann, I. R., Bortnik, J., Shao, L., & Angelopoulos, V. (2012). Themis observations of electromagnetic ion cyclotron wave occurrence: Dependence on ae, symh, and solar wind dynamic pressure. *Journal of Geophysical Research: Space Physics*, *117*(A10). Retrieved from <https://agupubs.onlinelibrary.wiley.com/doi/abs/10.1029/2012JA018049> doi: <https://doi.org/10.1029/2012JA018049>
- Usanova, M. E., Mann, I. R., Kale, Z. C., Rae, I. J., Sydora, R. D., Sandanger, M., ... Vallières, X. (2010). Conjugate ground and multisatellite observations of compression-related emic p<sub>c1</sub> waves and associated proton precipitation. *Journal of Geophysical Research: Space Physics*, *115*(A7). Retrieved from <https://agupubs.onlinelibrary.wiley.com/doi/abs/10.1029/2009JA014935> doi: <https://doi.org/10.1029/2009JA014935>
- Wygant, J. R., Bonnell, J. W., Goetz, K., Ergun, R. E., Mozer, F. S., Bale, S. D., ... Tao, J. B. (2013, Nov 01). The electric field and waves instruments on the radiation belt storm probes mission. *Space Science Reviews*, *179*(1), 183-220. Retrieved from <https://doi.org/10.1007/s11214-013-0013-7> doi: [10.1007/s11214-013-0013-7](https://doi.org/10.1007/s11214-013-0013-7)
- Xue, Z., Yuan, Z., Yu, X., Deng, D., & Huang, Z. (2022). Second-harmonic gen-

- eration of emic waves in the inner magnetosphere: Theoretical analyses and hybrid simulations. *Geophysical Research Letters*, 49(10), e2022GL098166. Retrieved from <https://agupubs.onlinelibrary.wiley.com/doi/abs/10.1029/2022GL098166> (e2022GL098166 2022GL098166) doi: <https://doi.org/10.1029/2022GL098166>
- Yin, Z.-F., Zhou, X.-Z., Hu, Z.-J., Yue, C., Zong, Q.-G., Hao, Y.-X., ... Manweiler, J. W. (2022). Localized excitation of electromagnetic ion cyclotron waves from anisotropic protons filtered by magnetic dips. *Journal of Geophysical Research: Space Physics*, 127(6), e2022JA030531. Retrieved from <https://agupubs.onlinelibrary.wiley.com/doi/abs/10.1029/2022JA030531> (e2022JA030531 2022JA030531) doi: <https://doi.org/10.1029/2022JA030531>
- Yu, X., Yuan, Z., & Xue, Z. (2021). Second-harmonic generation of electromagnetic emissions in a magnetized plasma: Kinetic theory approach. *Geophysical Research Letters*, 48(5), e2020GL091762. Retrieved from <https://agupubs.onlinelibrary.wiley.com/doi/abs/10.1029/2020GL091762> (e2020GL091762 2020GL091762) doi: <https://doi.org/10.1029/2020GL091762>
- Zhu, H., & Chen, L. (2019). On the observation of electrostatic harmonics associated with emic waves. *Geophysical Research Letters*, 46(24), 14274-14281. Retrieved from <https://agupubs.onlinelibrary.wiley.com/doi/abs/10.1029/2019GL085528> doi: <https://doi.org/10.1029/2019GL085528>